24th COBEM - 2017

24th ABCM International Congress of Mechanical Engineering
December 3-8, 2017, Curitiba, PR, Brazil

COBEM-2017-2057
CONVERSION OF SUPERELASTIC NiTi SMA WIRES IN THERMOMECHANICAL ACTUATORS: A STUDY BASED ON HEAT TREATMENTS

Daniel Jobson Alves Ribeiro
Paulo César Sales da Silva
Carlos José de Araújo
Emerson da Trindade Marcelino
Federal University of Campina Grande (UFCG), Rua Aprígio Veloso, 882, CEP 58429-140, Campina Grande – PB, Brazil
danielaeroufcg@gmail.com, engenheiropcsales@gmail.com, carlos.araujo@ufcg.edu.br, emerson.t.m.eng@gmail.com.

Abstract. *Shape Memory Alloys (SMA) are important smart materials that, after thermomechanical stimuli, present the phenomena of Shape Memory Effect (SME) and Superelasticity (SE). In both cases, large deformations can be recovered, upon heating for the SME and upon loading and unloading for the SE. NiTi SMA are currently employed in the medical and dental market in the form of tools and accessories for specific procedures. For these SMA, heat treatments are an adequate procedure for manipulating thermomechanical and functional (SME and SE) properties. Thus, this work aims to study the influence of annealing heat treatments on the thermomechanical behavior of NiTi SMA wires (originally superelastic). The factorial planning method was used to evaluate the influence of annealing temperature and time variables on some properties, as energy dissipation capacity, hardness, transformation temperatures, thermal hysteresis and transformation enthalpies. It was found that the annealing heat treatments carried out at 550°C are capable of converting NiTi SMA wires from the superelastic state to the actuator state, which was noticed by the occurrence of the Shape Memory Effect.*

Keywords: *Shape memory alloys; NiTi alloys; Heat treatments; Factorial planning.*

1. INTRODUCTION

Shape Memory Alloys (SMA) have arouse interest for the development of applications in the automotive, aeronautical, biomedical, naval and structural industries, among others. These smart metals exhibit a non-conventional thermomechanical behavior due to a specific adifusional solid-solid phase transformation between the austenite and martensite phases. The thermomechanical phenomena involved in these materials are the Shape Memory Effect (SME) and Superelasticity (SE). The first phenomenon allows to recover apparently plastic deformations after the mechanical loading and unloading of the SMA at a coldest state (martensite) followed by heating to the warmer phase, at a higher temperature (austenite). The second phenomenon, SE, in turn, occurs when the mechanical loading is applied in the austenite phase and the martensite phase is induced by mechanical stress causing large deformations that are recovered after the subsequent unloading, not presenting residual deformations. Among these materials, we highlight the Nickel-Titanium alloys (NiTi) whose composition approaches the equiatomic (Otsuka & Wayman, 1998). The medical and dentistry industries have a special interest in NiTi SMA due to its excellent biocompatibility and the ability to generate practically constant efforts at relatively large deformations (between 4% and 8%), a behavior observed in SE.

Recently, Grassi (2014) showed that annealing heat treatments in a temperature range between 350°C and 550°C with times varying from 20 to 180 minutes allow the manipulation of properties such as stiffness, energy dissipation, phase transformation temperatures and thermal hysteresis in NiTi SMA mini coil springs marketed for orthodontic purposes.

In this context, the main objective of this work is to present a mapping of thermomechanical properties of NiTi SMA wires, originally superelastic at room temperature (about 22 ºC), in such a way that it is possible to identify the viability of converting them into thermomechanical actuators (shape memory effect), with the intention of reducing material imports and developing new engineering applications.

2. MATERIALS AND METHODS

2.1 NiTi wires

For this work NiTi SMA superelastic wires with diameter of 0.4 mm, polished surface, supplied by Sandinox Biomaterials (São Paulo, Brazil) were used. From these wires, specimens with approximately 60 mm length were used to perform the heat treatments and thermomechanical characterization tests. These wires meet the requirements of ASTM F2063 that defines the quality standards for NiTi SMA used in medical devices and surgical implants.

2.2 Factorial planning

The annealing heat treatments were realized according to the planning matrix presented in Tab. 1. Two factors were established: temperature and annealing time, with two levels for each factor. This factorial planning is the same used by Grassi (2014).

Table 1. Experimental planning matrix used in this research to perform heat treatments.

Test	Temperature (°C)	Time(min)
1	300 (-1)	60 (-1)
2	300 (-1)	180 (+1)
3	550 (+1)	60 (-1)
4	550 (-1)	180 (+1)
5	250 (-1,41)	120 (0)
6	600 (1,41)	120 (0)
7	425 (0)	35 (-1,41)
8	425 (0)	205 (+1,41)
9	425 (0)	120 (0)
10	425 (0)	120 (0)
11	425 (0)	120 (0)

The variables of interest were evaluated using ANOVA (ANalysis Of VAriance), which is defined as a statistical method used to test the hypothesis that changes in the levels of each factor can cause changes in the response variable (Galdámez, 2002; Montgomery, 2008).

2.3 Thermomechanical characterization

The phase transformation temperatures of the NiTi SMA wires were determined by Differential Scanning Calorimetry (DSC) tests using a TA Instruments equipment, model Q 20. The tests were performed according to ASTM F2004-05, using a rate of 10 °C/min during heating and cooling, in a temperature range from -60 °C to 100 °C. Samples of NiTi wire with approximately 5 mm in length were used.

Isothermal loading and unloading tests were performed in uniaxial tensile mode. For this, the Instron universal electromechanical testing machine, model 5582, equipped with a thermal chamber for temperature control was used. The tests were realized at a temperature range from 30 to 90 °C, in intervals of 15 °C and until 10% of maximum deformation relative to the useful length of the wire specimens (20 mm) at a speed of 0.5 mm/min. Then, the evolution of the mechanical behavior as a function of temperature is obtained, allowing to estimate the stress increase coefficients, C^A and C^M (Lagoudas, 2008). Figure 1 show the experimental setup used to perform these isothermal tests.

Figure 1. Instron universal testing machine, model 5582, equipped with thermal chamber.

The influence of the heat treatments on the hardness of the NiTi wires were verified by Vickers indentations using a Shimadzu equipment, model DHU 211S. NiTi wire samples were mounted onto bakelite (cured at 175 ºC) to provide an adequate mechanical anchorage during the test. Five indentations were performed on each sample, with a load of 200 gf for 20 seconds. All tests were performed at a room temperature of approximately 22 °C.

3. RESULTS AND DISCUSSIONS

3.1 Thermal analysis

From the curves obtained by DSC, shown in Fig. 2, and applying the tangents method to the peaks, it was possible to determine the start, peak and finish critical temperatures of phase transformations. It were determined during cooling the martensite (M_s, M_f) and R-phase (R_s, R_f) temperatures while during heating the austenite (A_s, A_f) temperatures. These temperatures as well as the peak transformation temperatures, M_p, R_p and A_p, thermal hysteresis (ΔT_h) and phase transformation enthalpies (ΔH) are presented in Tabs. 2 and 3, respectively. In Tab. 2, the notation A_s'and A_f' (heating) is used for the case where only the partial transformation of austenite into R-phase.

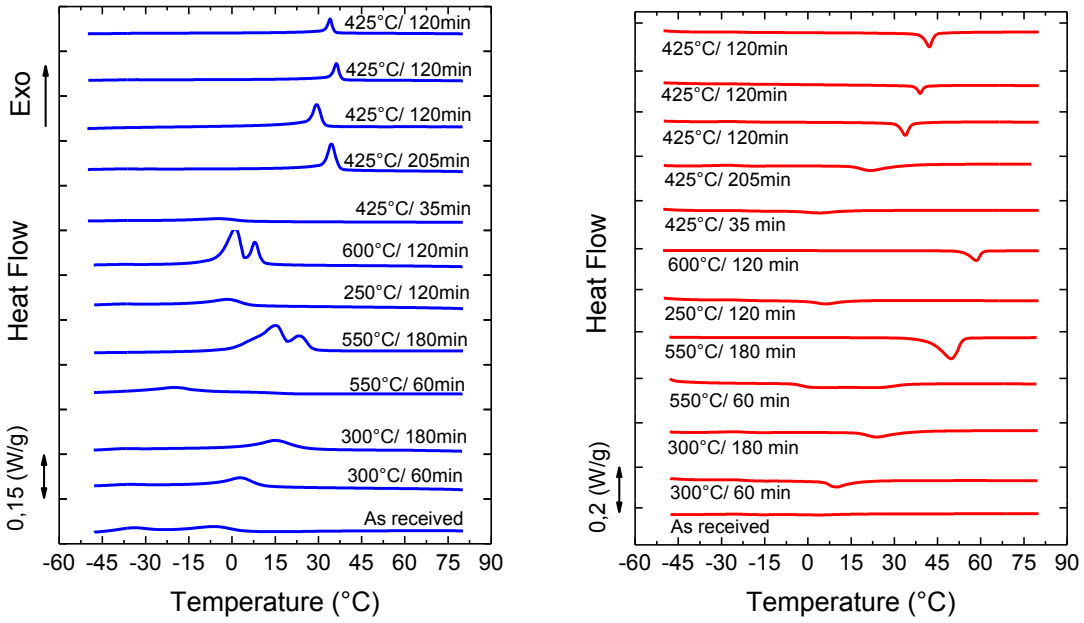

Figure 2. DSC curves for all the heat treatment conditions studied.

Table 2. Phase transformation temperatures for all heat treated NiTi wires.

Annealing conditions									
Temperature	**Time**	M_f	M_s	R_f	R_s	A_s'	A_f'	A_s	A_f
(°C)	(min)				(°C)				
As received		-	-	-15.34	5.46	-5.71	14.95	-	-
300	60	-	-	-6.88	11.40	5.20	18.44	-	-
300	180	-	-	4.81	25.62	12.69	22.53	-	-
550	60	-	-	-41.12	22.31	6.64	36.97	-	-
550	180	-0.12	18.98	18.98	27.90	-	-	41.90	54.30
250	120	-	-	-10.18	6.64	-1.12	14.73	-	-
600	120	-6.63	4.72	4.72	11.56	-	-	49.92	61.33
425	35	-	-	18.79	5.14	-4.74	11.56	-	-
425	205	-	-	29.46	38.52	37.39	46.53	-	-
425	120	-	-	24.47	32.86	29.46	36.63	-	-
425	120	-	-	34.28	38.15	38.48	42.68	-	-
425	120	-	-	30.21	37.01	35.88	42.37	-	-

Table 3. Thermal hysteresis and transformation enthalpies for heat treated NiTi wires.

Annealing conditions		**Enthalpy (ΔH)**						**Thermal hysteresis (ΔT_h)**	
T	***t***	***R→M***	***A→R***	***ΔH Total***	***M→A***	***R→A***	***ΔH Total***	***M-A***	***R-A***
°C	min	J/g						°C	
As received		-	1.59	1.59	-	1.77	1.77	-	9.49
300	60	-	3.18	3.18	-	2.98	2.98	-	7.14
300	180	-	3.61	3.61	-	3.22	3.22	-	9.65
550	60	-	3.04	3.04	-	3.18	3.18	62.64	28.52
550	180	6.67	2.41	9.08	15.86	-	15.86	34.83	32.38
425	120	-	3.21	3.21	-	3.64	3.64	-	4.72

From the results of Tabs. 2 and 3 it can be concluded that in most cases the observed phase transformations are in fact intermediate transformations (involving only the austenite and R-phase), except for the heat treatment conditions of 550 °C for 180 minutes and 600 °C for 120 minutes, where there were practically complete transformations. The main factors that led to this conclusion are the low thermal hysteresis, characteristic of the R-phase (Otsuka & Wayman, 1998), which was of the order of 7.75 °C (mean value), and the low values of transformation enthalpies (ΔH = 2.90 J/g). It is well known that transformation of the R-phase (A – R) releases low energy when compared to the complete martensitic transformation (A – M), which presents typical enthalpy values between 15 and 35 J/g (Meschel et al, 2011; Otubo et al, 2008; Otsuka and Wayman, 1998). When the NiTi SMA is heat treated at more higher temperatures (550 °C and 600 °C), the peak of the R-phase transformation tends to overlap with the peak of the martensite, leading to a direct transformation of the austenite to the martensite during cooling. In addition, these treatments at 550 °C for 180

minutes and 600 °C for 120 minutes were able to increase the transformation temperatures, such that, at room temperature, the NiTi wires come to present the SME. The heat treatment time also maintained a direct proportional relationship with these temperatures, increasing them as the wires were treated for longer periods, increasing the thermal hysteresis of the R-phase.

From the data summarized in Tabs 2 and 3 and using factorial planning, it was possible to obtain statistical mathematical models to predict these properties with changes in time and temperature of annealing. For the generation of a mathematical model that well describes the behavior of R_s temperature it was necessary to use a quadratic factorial planning, where 11 experiments are performed. The other evaluated properties (ΔT_h, A_f and ΔH) were well described by the models obtained with the linear experimental planning, where only 4 experiments were necessary. In Fig. 3, the previously mentioned behaviors are confirmed interpreting the level curves for the thermal hysteresis (A_p - R_p) and for the enthalpy of the transformation $A \rightarrow R$ (cooling), respectively. Figure 4 shows the behavior of the transformation temperatures R_s and A_f while Tab. 4 allows to verify the ANOVA result applied to the experimental planning performed for all properties.

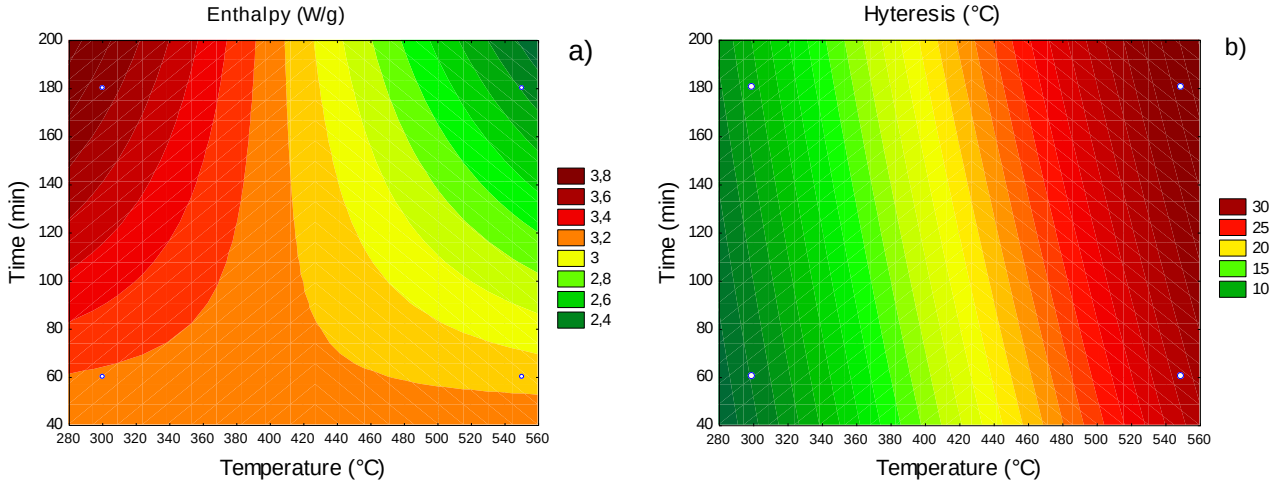

Figure 3. Level curves for thermal hysteresis ($\Delta T_h = A_p' - R_p$) (a) and transformation enthalpy of the R-phase (ΔH_{A-R}) (b), both obtained by linear experimental planning.

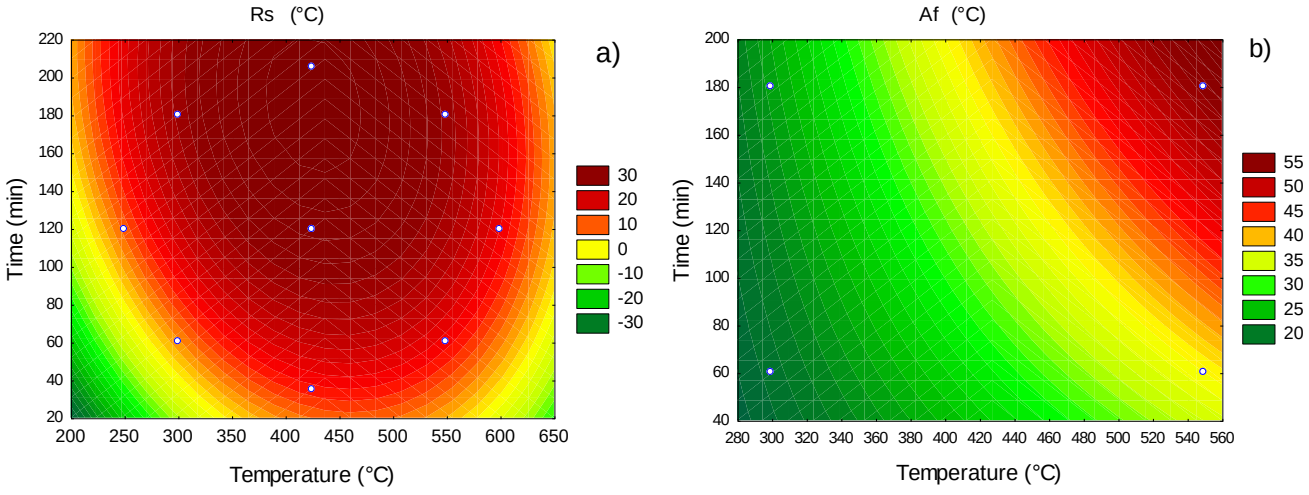

Figure 4. Level curves for phase transformation temperatures R_s (a) and A_f (b), obtained by a quadratic and linear planning, respectively.

Table 4. Results of the ANOVA analysis concerning the responses for ΔT_h and $\Delta H_{A\text{-}R}$.

Properties	*Factors*	R^2	*P-value*	$F_{calculated}$	*Minimum degree of confidence(%)*
Hysteresis (ΔT_h)	Temperature (*T*)	0.99	0.000003	1453.94	99.05
	Time (*t*)		0.000001	3216.39	99.05
	*T***t*		0.000109	231.13	99.05
Enthalpy ($\Delta H_{A\text{-}R}$)	Temperature (*T*)	0.98	0.000098	243.77	99.05
	Time (*t*)		0.009191	238.84	99.05
	*T***t*		0.001886	210.08	99.00
A_f	Temperature (*T*)	0.99	0.000000	19241.56	99.50
	Time (*t*)		0.000000	3511.91	99.50
	*T***t*		0.000003	1393.83	99.50
R_s	Temperature (L)	0.92	**0.319056**	**1.22**	<90.00
	Temperature (Q)		0.006596	19.95	97.50
	Time (L)		0.012238	**14.67**	95.00
	Time (Q)		**0.095689**	**4.40**	90.00
	T(L)**t*(L)		**0.481575**	**0.57**	<90.00

In Table 4 it is possible to verify that the lowest values obtained for R^2, that represents the degree of adjustment of the obtained model, occurred for the variable R_s, being approximately 92%, and reaching 99% for A_f and for the ΔT_h, confirming that the mathematical models obtained are sufficiently well adjusted. In the case of R_s for which the adjustment factor was 92%, there is a region where the phenomenon is not well represented by the obtained model. The P-value had its maximum plots highlighted for R_s factors, being possible to affirm that the probability of failing to assume the influence of the quadratic temperature (Q) and linear time (L) plots on the response is minimal, while for the other factors there is great chance of error.

The other evaluated properties presented a P-value that was sufficiently low for all the factors, proving their influence on the responses. In the F-test, it can be verified that the $F_{calculated}$ for the factors and interaction between factors of all properties is greater than the $F_{tabulated}$ = 7.71 for a confidence level of 95%, except for R_s. Thus, it is possible to affirm that the response variable was influenced sufficiently by changes in factor level, not due to random and uncontrollable causes. For the cases where the $F_{calculated}$ of the factors are greater than four times the values of $F_{tabulated}$, it is possible to affirm that the obtained mathematical model is also predictive. This condition was satisfied in all properties evaluated for a 95% confidence level, except for R_s, where it was only satisfied for a 90% of confidence level for the temperature (Q) factor. This means that the mathematical model obtained for R_s, although not providing extremely accurate results, provides acceptable values, providing better values in regions near the center of the level curves.

3.2 Mechanical Behavior at Different Temperatures

In Figures 5 and 6 it is possible to observe qualitatively as well as quantify the behavior of the critical transformation stresses through the determination of coefficients that represent the increase of these stresses as a function of temperature. This behavior corresponds to a Clausius-Clayperon's law for SMA (Otsuka & Wayman, 1998) and can be observed in Fig. 7.

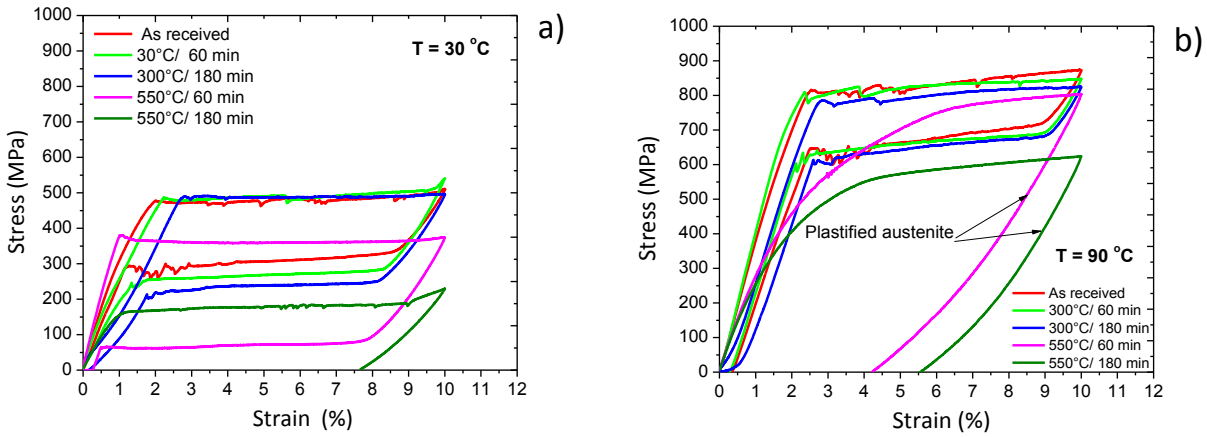

Figure 5. Thermomechanical behavior of the NiTi wires for different heat treatment conditions (a) Test temperature of 30 ° C. (b) Test temperature of 90 °C.

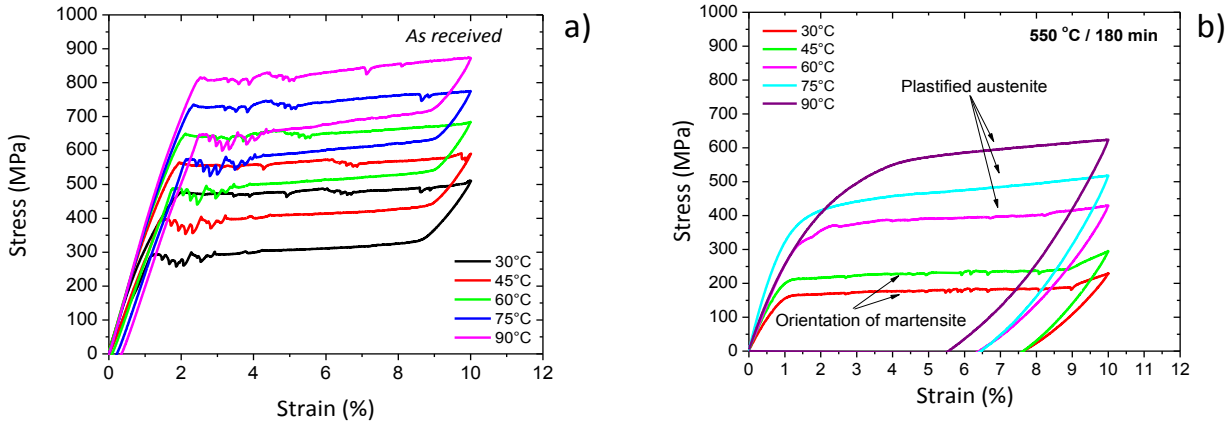

Figure 6. Thermomechanical behavior of the NiTi wires as a function of the test temperature. (a) Wire without heat treatment. (b) Wire heat treated at 550 °C for 180 minutes.

It is possible to observe from these figures that the heat treatments at 550 °C were able to change considerably the behavior of the NiTi wire. The wires initially presenting a SE behavior were converted to present the SME, as observed by the residual deformation of more than 7% for 30 °C (Figs. 5a and 6b). This residual deformation can be recovered by heating, characterizing the SME behavior.

Fig. 6(a) shows that the stress required to generate 10% deformation increases proportionally to the test temperature. This phenomenon occurs due to the fact that the austenite phase is more stable at high temperatures and to induce martensitic transformation it is necessary to apply more mechanical energy to the system. This behavior is at the origin of Clausius-Clapeyron's law for SMA (Otsuka and Wayman, 1998). It can be seen in Fig. 6(b) that the mechanical behavior for heat treatments at 550 °C for 60 and 180 minutes tested at higher temperatures (above A_f) presented a greater residual deformation, which is a typical behavior of tests performed above the temperature M_d. In this temperature plastic deformation of austenite occurs before there is stress-induced martensite formation. The critical stress for martensite formation becomes greater than the stress required to cause plastic deformation by the movement of dislocations (Miyazaki et al., 1981). This behavior does not occur with the wire that has not undergone any heat treatment (as received wire, Fig. 6a) showing that the martensite was induced by stress without occurrence of plastic deformation of the austenitic matrix.

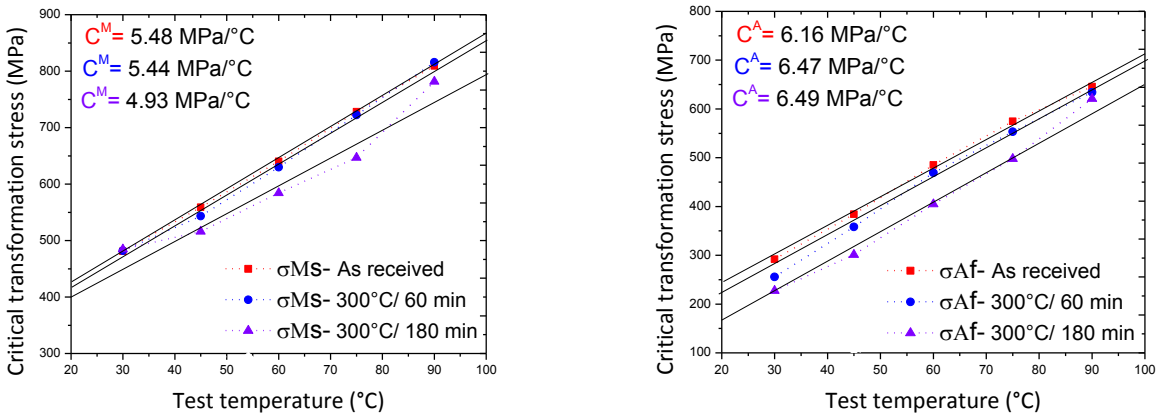

Figure 7. Transformation stresses as a function of test temperatures for the NiTi SMA wire.

The dissipated energy (E_D) in each thermomechanical superelastic cycle (Fig. 6a, for example) were calculated as the internal area of the force versus displacement loops. Table 5 shows the E_D results of the NiTi wires for the studied annealing conditions in which the superelasticity was maintained, as a function of the test temperature.

Table 5. E_D values obtained for all heat treatment conditions that maintains the SE phenomenon of the NiTi wires.

Test (°C)	**Temperature** (min)	**Time**	***E*D (MJ/m³) for all Test Temperatures**				
			30°C	**45°C**	**60°C**	**75°C**	**90°C**
1	As received		14.16	12.97	12.58	13.88	15.33
2	300	60	17.36	14.64	14.19	14.27	15.40
3	300	180	18.85	16.22	14.43	13.74	13.65
6	425	120	32.54	25.89	22.98	21.65	20.27

The dissipated energy is closely related to the degree of atomic mobility in the crystalline lattice during phase transformation. In Fig. 8, which shows the variation of E_D with the heat treatment conditions and the test temperature, it is possible to notice that the lower energy dissipated levels were observed in the wire that received no any heat treatment. Heat treatments up to 300 °C, independently of the duration, practically did not contribute significantly to the recovery of the atomic mobility, resulting in a minimum increase of E_D in relation to the condition of the wire as received. With increasing heat treatment temperatures up to 425 °C, a proportional increase of E_D was observed.

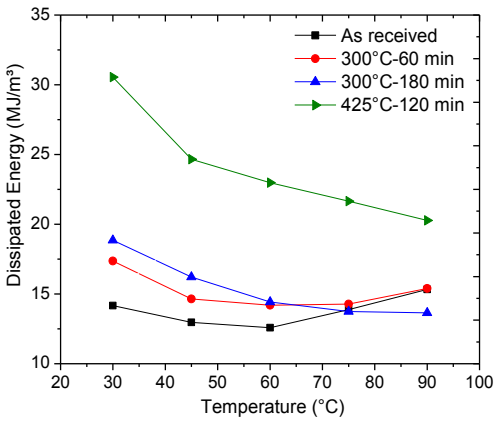

Figure 8. Dissipated energy (E_D) by the NiTi SMA wires as a function of the test temperature for the heat treatment conditions that maintains superelasticity.

3.3 Hardness

The hardness values for all the conditions evaluated in this work are presented in Tab. 6. It can be observed the determined hardness in each of the five indented points and their respective mean value and standard deviation (SD). In Fig. 9(a) it is possible to verify the behavior of the hardness in a qualitative way, clearly perceiving how the heat treatment realized at 550 °C and 180 minutes promoted a greater reduction in the hardness, decreasing from 469 HV (as received) to about 291 HV. In Fig. 9(b) it is possible to visualize the mark left by the pyramidal indenter, from which the hardness value based on its dimensions is calculated.

Table 6. Hardness values for all heat treatment conditions of the NiTi SMA wire.

Test	**Temperature** (°C)	**Time** (min)	**Hardness (HV)**					
			1	2	3	4	5	**Mean ± SD**
1	300	60	457.25	470.95	460.18	475.31	442.14	**461.16 ± 12.98**
2	300	180	480.38	439.28	431.91	444.84	463.13	**451.90 ± 19.65**
3	550	60	399.73	402.11	370.42	400.68	382.15	**391.01 ± 14.09**
4	550	180	288.32	276.66	305.18	292.84	289.91	**290.58 ± 10.21**
5	425	120	370.45	420.98	362.16	390.57	445.97	**398.02 ± 35.09**
6	As received		430.92	467.36	490.85	472.38	487.12	**469.72 ± 23.80**

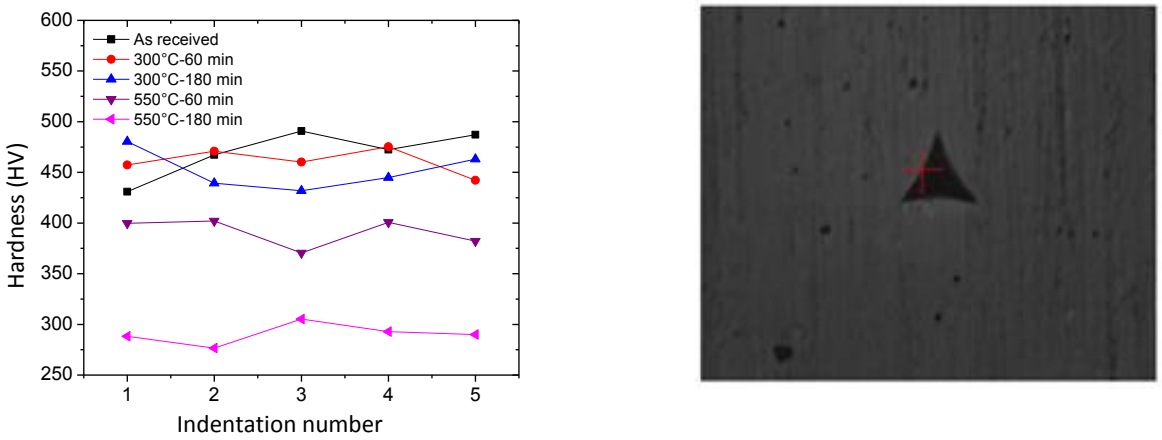

Figure 9. Hardness behavior of the NiTi wire for the heat treatments used. (a) Hardness values in five tests. (b) Indentation image on polished surface of NiTi wire.

Based on these results, it is observed that the hardness of the heat treated NiTi wires at higher temperatures and times decreases. In the literature, it is possible to find hardness values that vary between 365 HV and 450 HV for the material without heat treatment (Catão et al., 2012).

4. CONCLUSIONS

From the ANOVA analyzes performed in this work it was possible to verify that the heat treatment temperature (annealing) is the factor of greater influence on the phase transformation and thermomechanical behavior of the superelastic NiTi SMA wire studied. The time showed to be important in the variation of the transformation temperatures, however it had little contribution in relation to changes in the enthalpy of the R-phase transformation ($A \rightarrow R$).

Concerning the annealing temperatures, it was concluded that up to 300 °C the effects on the studied properties are due to the phenomena of stress-relief. Then, for these relatively low temperatures the changes observed in the material were not significant. Temperatures of 550 °C resulted in the reduction of the critical transformation stresses, since the microstructure was no longer totally austenitic, but partially R-phase or martensitic. The same effect was observed in

the hardness of the material, which decreased considerably, while the dissipated energy increased due to the greater atomic mobility acquired by the NiTi wires**.**

These heat treatments were also able to increase considerably the transformation temperatures, leading to the appearance of the transformation peak of the martensite phase, this being merged with the peak of the R-phase in the cooling. This behavior caused the NiTi SMA wire to exhibit the shape memory effect after deformation at room temperature and subsequent heating.

Finally, it is possible to affirm that an element of NiTi SMA initially designed to work in superelastic regime, can be converted into actuating element to work in regime of shape memory effect, being able to be applied in several engineering applications.

5. ACKNOWLEDGEMENTS

The authors thank the CNPq Brazilian Agency for funding the following research projects: INCT of Smart Structures for Engineering (grant number 574001/2008-5), PQ-1D (grant number 304658/2014-6) and Universal 01/2016 (grant number 401128/2016-4).

6. REFERENCES

ASTM 2004-05: Standard Test Method for Transformation Temperature of Nickel-Titanium Alloys by Thermal Analysis. Accessed in: 12/10/2017**,** available in www.astm.org.

ASTM 2063: Standard Specification for Wrought Nickel-Titanium Shape Memory Alloys for Medical Devices and Surgical Implants. Accessed in: 12/10/2017**,** available in www.astm.org.

Catão, C. D. S; Lia Fook, M. V; Rabello, I. P.; Fook, A. C. B. M.; de Araújo, C. J.; Vilar, Z. T.; 2012. "Obtainment and evaluation of NiTi alloys laser treated coated with apatite for use in dental implants". *In Proceedings of the Latin American Congress of Artificial Organs and Biomaterials – COLAOB2012*. Natal, Brazil.

Galdámez, E. V. C., 2002. *Aplicação das Técnicas de Planejamento e Análise de Experimentos de Melhoria da Qualidade de um Processo de Fabricação de Produtos Plásticos*. MSc Thesis, Escola de Engenharia de São Carlos da Universidade de São Paulo, São Carlos, Brazil.

Grassi, E. N. D., 2014. *Comportamento Termomecânico de Mini Molas Superelásticas de NiTi: Influência de Tratamentos Térmicos*. MSc Thesis, Universidade Federal de Campina Grande (UFCG), Campina Grande, Brazil.

Lagoudas, D. C., 2008. "Shape Memory Alloys: Modeling and Engineering Application". Edited by Lagoudas, D. C., Springer, Texas, USA. ISBN 978-0387-47685-8.

Meschel, S. V., Pavlu, J., Nash, P., 2011. "The Thermochemical Behavior of Some Binary Shape Memory Alloys by High Temperature Direct Synthesis Calorimetry". *Journal of Alloys and Compounds*, Vol. 509, Number 17, pp 5256–5262.

Miyazaki, S.; Otsuka, K.; Suzuki, Y., 1981. "Transformation pseudoelasticity and deformation behavior in Ti-50.6at%Ni alloy". Scripta Metallurgica, Vol.15, p287-292.

Montgomery, D. C., 2008. "Design and Analysis of Experiments". 7th ed. Hoboken: J. Wiley. ISBN 1118146921.

Otsuka, K.; Wayman, C. M., 1998. "Shape Memory Materials.". Cambridge University Press, 1st edition.

Otsuka, K.; Ren, X., 1999. "Martensitic transformations in nonferrous shape memory alloys". *Materials Science and Engineering A*, v. 273-275, p. 89-105.

Otubo, J.; Rigo, O. D.; Coelho, A. A.; Neto, C. M.; Mei, P. R.; 2008. "The influence of carbon and oxygen content on the martensitic transformation temperatures and enthalpies of NiTi shape memory alloy". *Materials Science and Engineering A*, Vols. 481-482, pp 639–642.

7. RESPONSIBILITY NOTICE

The authors are the only responsible for the printed material included in this paper.